Organic & Biomolecular Chemistry

PAPER

View Article Online
View Journal

Cite this: DOI: 10.1039/c5ob01594d

Identification of noreremophilane-based inhibitors of angiogenesis using zebrafish assays†

Kalai Mangai Muthukumarasamy,‡[a] Kishor L. Handore,‡[b,c] Dipti N. Kakade,[b] Madhuri V. Shinde,[b] Shashi Ranjan,[a] Naveen Kumar,[d] Seema Sehrawat,[d] Chetana Sachidanandan*[a] and D. Srinivasa Reddy*[b,c]

Received 31st July 2015,
Accepted 8th October 2015

DOI: 10.1039/c5ob01594d

www.rsc.org/obc

Noreremophilanes are a rare class of *cis*-hydrindanes produced by genus *Ligularia* herbaceous plants which are known to exhibit interesting biological activities. We synthesized *cis*-hydrindanes based on a naturally occurring noreremophilane scaffold using a Diels–Alder/aldol sequence and screened them for multiple biological activities using high-content zebrafish embryonic development assays. We discovered a noreremophilane that has strong anti-angiogenic effects on the developing zebrafish embryos as well as on tumor-induced angiogenesis in a zebrafish xenograft model. We synthesized several derivatives of this class of noreremophilanes and performed structure–activity relationship studies in zebrafish to identify more potent and less toxic analogs of the original structure.

Introduction

Nature is an abundant and underexplored source of small molecules with a variety of bioactivities. Many of these small molecules when taken out of their context and applied on live cells yield unexpected and potentially useful activities.[1] Among natural products certain scaffolds are found to reoccur in several species, but studying their activities remains a challenge due to the miniscule quantities that can be extracted from their natural source. Moreover, the discovery of new bioactivities necessitates multiple assays to hunt for therapeutically important activities. Here we circumvent these challenges by synthesizing derivatives of natural-product-based scaffolds and testing them using whole-organism assays in zebrafish embryos. Zebrafish has emerged as an ideal model organism that is accessible for high throughput assays while being complex enough to model the vertebrate biology.[2,3] A number of recent studies have illustrated the power of whole-organism screening in zebrafish to identify unexpected bioactivities of small molecules.[4,5]

The *cis*-hydrindane backbone has been extensively used in nature, in particular in sesquiterpenoids.[6] The *cis*-hydrindane motifs are found in many natural products with known biological activities.[6,7] For example, peribysin-E **1** (Fig. 1), isolated from marine organisms was shown to be a potent cell adhesion inhibitor with potential for use as anti-inflammatory and anti-cancer agents.[8] Bakkenolides **2** and **3** are another interesting family of natural products (Fig. 1) with multiple bioactivities.[9,10] Similarly noreremophilane-type sesquiterpenes **4–6** also contain the *cis*-hydrindane framework which were isolated from the roots of *Ligularia* herbaceous plants. Some of these have attracted our attention previously due to

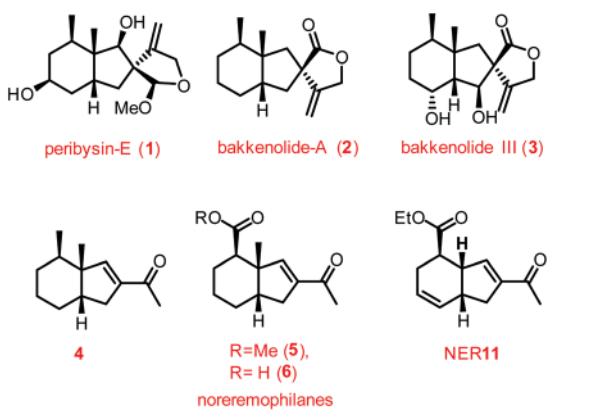

Fig. 1 Selected natural products with the *cis*-hydrindane skeleton.

[a]*CSIR-Institute of Genomics & Integrative Biology (CSIR-IGIB), South Campus, New Delhi, 110025, India. E-mail: chetana@igib.in*
[b]*CSIR-National Chemical Laboratory (CSIR-NCL), Division of Organic Chemistry, Dr Homi Bhabha Road, Pune, 411008, India. E-mail: ds.reddy@ncl.res.in*
[c]*Academy of Scientific and Innovative Research (AcSIR), 110025 New Delhi, India*
[d]*Vascular Biology Lab, Department of Life Sciences, School of Natural Sciences, Shiv Nadar University, India*

†Electronic supplementary information (ESI) available: Characterization data, NMR spectra, detailed experimental procedures, and CIF file of X-ray crystal structures. CCDC 1009597. For ESI and crystallographic data in CIF or other electronic format see DOI: 10.1039/c5ob01594d

‡Both authors contributed equally.

their interesting biological activity and feasibility in accessing several molecules using the methods we have developed previously.[11–13]

In the present work we discovered a noreremophilane based on the natural *cis*-hydrindane backbone that is a potent angiogenesis inhibitor. The noreremophilane **11** (known as NER**11** from here on) appears to inhibit angiogenesis in normal zebrafish embryos as well as in human endothelial cell cultures.

Angiogenesis is the formation of new blood vessels from the pre-existing ones and is a process essential for both physiological and pathological events. Blood vessels bring oxygen and nutrients to the cells, remove waste from tissues and are the major communication link between different tissues within the body. The functional blood vessel is comprised of endothelial cells that form the lumen to carry blood, surrounded by a variety of cell types that provide support to the fragile vessel. Angiogenesis is a complex process, the result of signals from the surrounding milieu to the endothelial cells, secretion of extracellular matrix degrading enzymes such as matrix metalloproteases (MMPs) and mobilization of the endothelial cells that finally leads to the sprouting of new blood vessels.[14]

Excessive angiogenesis is closely related to many human diseases such as tumor growth, retinopathy and inflammation.

In cancerous growth, the tumor secretes pro-angiogenic factors, in particular vascular endothelial growth factor (VEGF) and basic fibroblast growth factor (bFGF), that stimulate angiogenesis so that the nutrient demands of a growing tumor can be met. Increased angiogenesis correlates with a poor prognosis as well as decreased overall survival of the patient.[15] Anti-angiogenesis therapy aims at inhibiting angiogenesis in the tumor environment, thus starving the tumor of oxygen and nutrients. This idea was developed around the 1990s by researchers such as Judah Folkman, who proved angiogenesis is needed for tumor growth. Today, nearly one half of the novel drugs in anti-cancer clinical trials are angiogenesis inhibitors rather than cytotoxic agents.[16]

Using a zebrafish xenograft model we also show that NER**11** inhibits tumor-induced angiogenesis *in vivo*. Further, we synthesized a series of derivatives of NER**11** to identify the active moieties in the structure that are responsible for the anti-angiogenic activity. We discovered a number of different analogs that retain the angiogenesis-inhibitory activity while reducing their general toxicity for the embryo. Thus, we propose that *in vivo* whole organism screens in zebrafish are highly informative and can be used for identifying novel bioactive compounds and for studying their structure–activity relationship.

Results and discussion

Noreremophilane 11 inhibits angiogenesis and perturbs patterning of vasculature in zebrafish

From an initial screen in wild-type zebrafish embryos, we identified a potent bioactive compound, noreremophilane **11** (NER**11**). We characterized the effect of NER**11** on the embryonic zebrafish in detail. Embryos were treated with a concentration range of NER**11** (6.25 μM, 12.5 μM, 25 μM, 50 μM and 100 μM) at very early stages of development (6 hours post-fertilization) to assess its teratogenic effects. We found that at 25 μM the gross development of the embryos is normal. We also tested the expression of markers of the germ layer specification and gastrulation, important events in embryonic development, using RNA *in situ* hybridization in 10 somite stage embryos and found no remarkable changes in the NER**11** treated embryos compared to DMSO treated vehicle controls (Fig. S3†). Although apparently normal earlier, the embryos later developed tail curvature (Fig. S2†) and sluggish blood flow by 2 days post-fertilization (dpf), suggesting underlying molecular defects. The *Tg(myl7:Gal4-VP16)* transgenic zebrafish embryos, that express green fluorescent protein (GFP) in the heart, was used to assess heart defects. NER**11** treated embryos showed that the heart tube was elongated and did not loop correctly to form the two chambers: atrium and ventricle (Fig. S2†).

We visualized the blood flow using the *Tg(gata1a:DsRed)* transgenic line which expresses red fluorescence in the erythrocytes of blood (Fig. 2g). The NER**11** treated embryos had compromised blood flow and a significant accumulation of blood in the brain indicating blood vessel hemorrhage (Fig. 2h). This made us wonder if the vasculature in the brain is affected and we tested NER**11** on an endothelial marker transgenic line *Tg(flk1:EGFP)*; this line marks the blood vessels with GFP fluorescence. We observed that the main vessels of the brain were normal in compound-treated fishes but the dense meshwork of blood vessels in the brain were severely reduced indicating changes in the brain vascular patterning (Fig. 2i and j). Since angiogenesis is regulated by the vascular endothelial growth factor (VEGF) and its receptors, we visualized the expression of *flk1* (or *VEGFR2*) in the brain by RNA *in situ* hybridization. NER**11** caused a severe reduction in the *flk1* gene expression in the brain compared to vehicle treated control embryos indicating strong inhibitory effects on angiogenesis regulatory genes (Fig. 2k–n).

A standard assay for angiogenesis in zebrafish is to visualize the sub-intestinal vessel (SIV) formation after treatment with compounds. The main arteries and veins in the zebrafish embryo, the dorsal aorta and the posterior cardinal vein, respectively, are formed by 2 days of development. This process is called *de novo* vasculogenesis. Angiogenesis is the process of sprouting new blood vessels from the existing vessels. SIVs sprout from the major vessels between 2 and 3 days. We used *Tg(fli1:EGFP)* to visualize the blood vessels and treated 2-day-old embryos with different concentrations of NER**11** to assay angiogenesis. Control treated zebrafish embryos show a fan-shaped array of SIVs at 3 days (Fig. 2a and b). Embryos exposed to NER**11** showed a dose-dependent inhibition of SIVs (Fig. 2c–f).

NER11 inhibits tumor angiogenesis in zebrafish

To test whether the compound affects tumor angiogenesis also, we performed a xenotransplantation assay of cancer cells

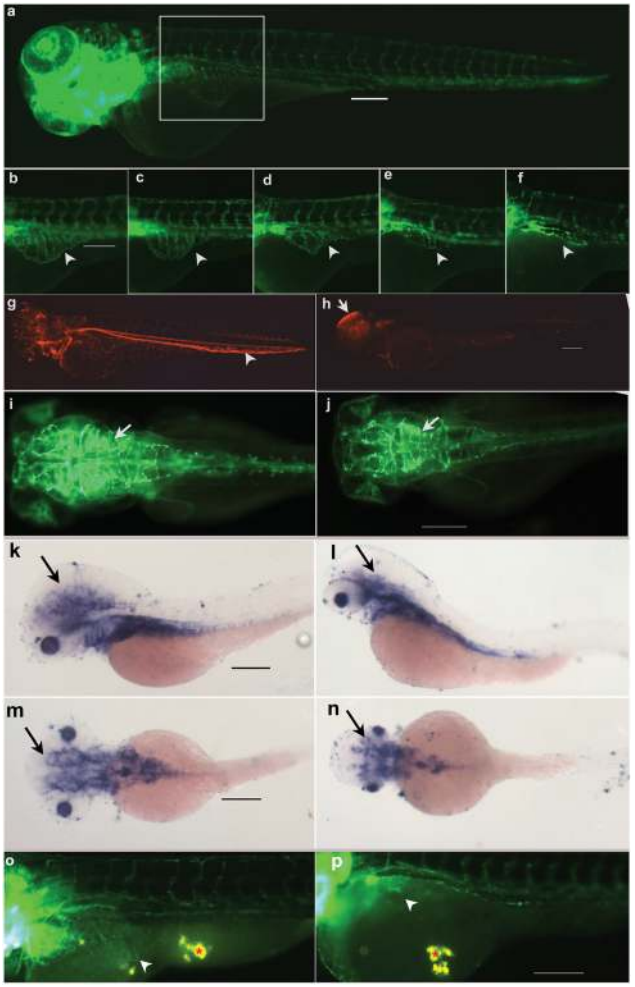

Fig. 2 Noreremophilane scaffold inhibits angiogenesis in zebrafish embryos. (a–f) Formation of subintestinal vessels (SIV) was analyzed for the anti-angiogenesis assay in zebrafish embryos. In the *Tg(fli1:EGFP)* zebrafish embryo (a), the rectangular box is the region showing SIV fan-shaped vessel formation which is magnified in (b–f, o and p). Two-day-old zebrafish embryos were treated with DMSO (a and b), 6.25 μM (c), 12.5 μM (d), 25 μM (e) and 50 μM (f) of NER**11** and imaged at 3 days. In NER**11** treated *Tg(fli1:EGFP)* zebrafish embryos SIVs were inhibited (c–f) in a dose-dependent manner compared to DMSO (b). (g and h) In *Tg(gata1a:DsRed)* red-labeled erythrocytes show normal blood flow highlighting the major blood vessels in DMSO treated embryos (arrowhead, g), whereas NER**11** treated embryos show interrupted flow and intracranial hemorrhage (arrow, h). To check for the effect of NER**11** on brain vasculature, *Tg(flk1:GFP)* embryos were treated with DMSO which show an intricate mesh of blood vessels in the brain (arrow, i), while NER**11** treated embryos have a reduced network of cranial blood vessels (arrow, j). RNA *in situ* hybridization for flk1 (VEGFR2) RNA expression in 3-day-old zebrafish embryos shows that DMSO treated embryos (k, m) have dense blood vessels in the brain (arrow) while compound **16** treated embryos have a much reduced network of cranial vessels (arrow, l and n). 2-day-old *Tg(fli1:EGFP)* embryos injected with MDA-MB-231 cancer cells near the SIV and then exposed to DMSO have a thick network of blood vessels perfusing the tumor mass (red asterisk) buried deep in the yolk (arrowhead, o) while SIVs were severely inhibited in NER**11** treated cancer-injected embryos (arrowhead, p). Excitation/emission wavelength used for GFP (a–f, i and j, o and p) was 495 nm/519 nm and for dsRed (g and h) was 565 nm/606 nm respectively. In all the images head of the embryos is to the left; lateral view (a–h, k and l, o and p) and dorsal view (i and j, m and n). Scale bars are 200 μm.

in zebrafish embryos. This assay has been used previously to identify inhibitors of tumor angiogenesis in zebrafish.[29] DiI-labeled MDA-MB-231 human breast cancer cells were injected near the perivitelline space of 2-day-old *Tg(fli1:EGFP)* zebrafish embryos and then the tumor mass was allowed to grow for 24 hours at 32 °C. We found that the xenografted embryos had prolific sprouting of blood vessels that burrowed deep towards the injected cell mass such that even visualizing their spread was made difficult (Fig. 2o). In contrast the NER**11** injected xenotransplanted embryos had a severely compromised vessel growth that did not reach the tumor mass (Fig. 2p) suggesting that the compound is capable of inhibiting pathological angiogenesis as well as normal developmental growth of vessels.

Synthesis and characterization of NER11 and related noreremophilanes

In order to identify the active moieties in NER**11** and to improve the activity to toxicity ratio, we synthesized a number of related noreremophilane derivatives. We used the Diels–Alder/aldol sequence to construct *cis*-hydrindanes. The dienophiles **7**, **8** and diene used for the present purpose were prepared using known procedures and they were subjected to the Diels–Alder[17–23] reaction in the presence of $BF_3{\cdot}Et_2O$ in dichloromethane solvent to give adduct **9**. The Diels–Alder adduct **9** was subjected to intramolecular aldol condensation reaction by exposing it to 15% KOH in ethanol to furnish NER**11** along with varying amounts of the corresponding carboxylic acid **13** (Scheme 1). The Lewis acid mediated intermolecular Diels–Alder reaction produced the *endo*-adduct having the aldol partners (*i.e.*, aldehyde and ketone) in close distance that allowed intramolecular aldol reaction in a facile manner to give *cis*-hydrindanes **11**/**13**. The observed high diastereo- and regioselectivity can be explained on the basis of secondary orbital interactions and atomic coefficient preferences, respectively.[24–27] By following the same protocol, compounds **12** and **14** were prepared in which the angular hydrogen atom was replaced with a methyl group. The isolated double bond in **12** on chemoselective reduction using Wilkinson's catalyst under a hydrogen atmosphere followed by ester hydrolysis using $LiOH–H_2O$ in ethanol furnished the target compound **6** in 72% isolated yield. Compound **14** on esterification with MeOH using the standard procedure afforded compound **15** which on reduction of the isolated double bond using Wilkinson's catalyst gave the natural product **5** in 70% yield. All the spectral data (IR, ^1H and ^{13}C NMR) for both natural products were found to be identical to those reported in the literature.[7,28] Towards the generation of a library of compounds around natural products, the carboxylic acids **13** and **14** were coupled with appropriate alcohols and amines which afforded the corresponding analogs **5** to **25**. In addition, selected compounds were prepared in an enantiopure form to understand the role of stereochemistry in activity. For this purpose, compound **13** was chosen and treated with D-(−)-pantolactone using standard coupling conditions to obtain a mixture of diastereomers **29a** and **29b** which are

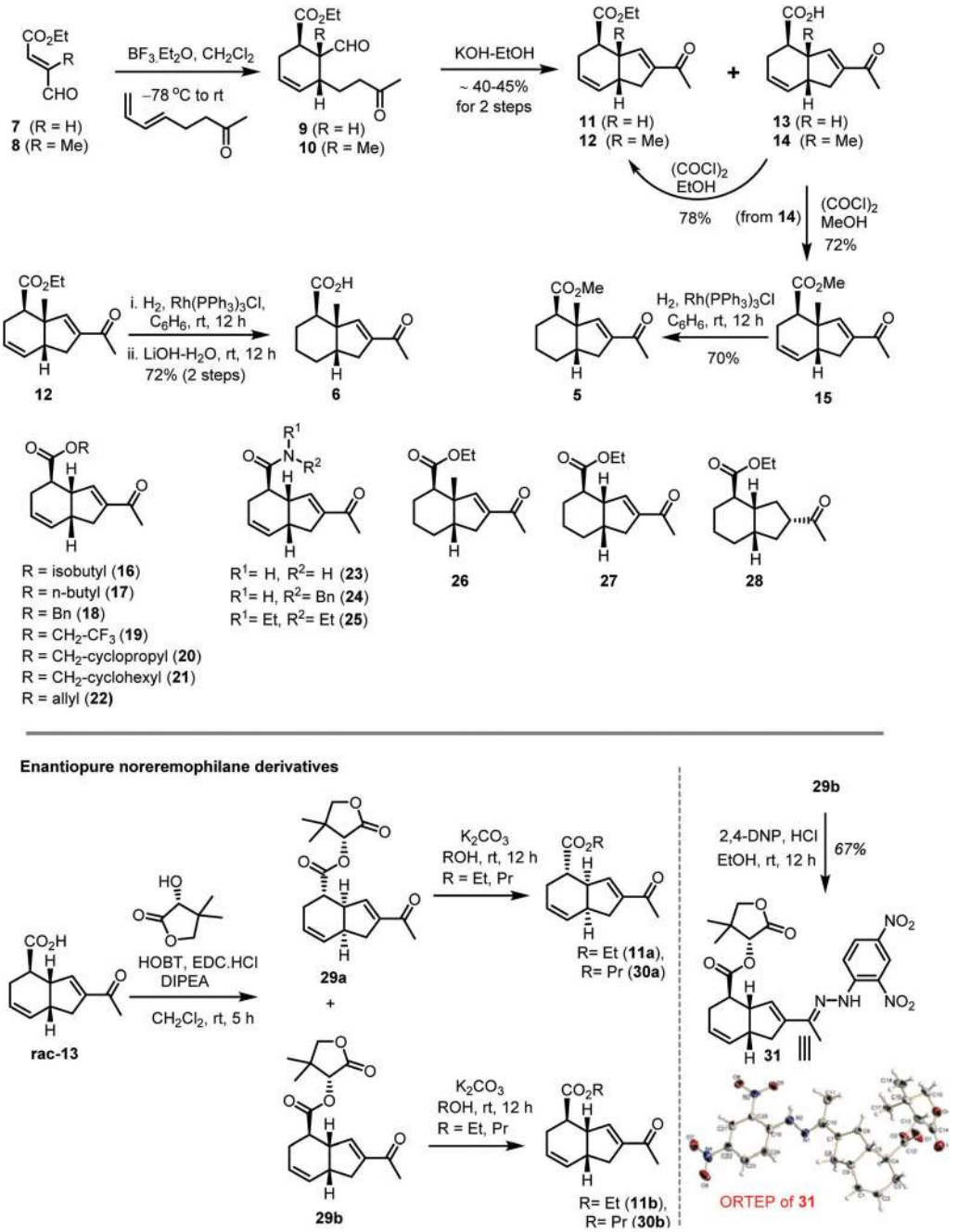

Scheme 1 Synthesis of noreremophilane based *cis*-hydrindanes.

cleanly separated by silica gel column chromatography. The trans-esterification using EtOH/PrOH, K_2CO_3 conditions gave the corresponding two enantiomers **11a**/**30a** and **11b**/**30b**. At this stage, we were interested in establishing the relative and absolute configurations of the synthesized enantiopure noreremophilane derivatives. Towards this effort, one of the pure enantiomers **29b** was treated with 2,4-DNP in EtOH to provide its 2,4-DNP derivative **31** as a crystalline solid. Compound **31** was recrystallized using ethyl acetate–hexane. Analysis of single crystal X-ray established the relative and absolute configurations as drawn in Scheme 1. Accordingly, all other enantiopure hydrindane configurations were derived as drawn in Scheme 1.

Structure–activity relationship (SAR) studies of the noreremophilane series using zebrafish developmental assays

All the synthesized derivatives of NER**11** were screened on zebrafish embryos. Two independent assays were performed: (1) for anti-angiogenesis activity and (2) for teratogenic activity. Teratogenicity was assayed in 1-day old embryos while angiogenesis was assayed in 2–3-day-old embryos. Both the assays were performed at 50 μM concentration of compounds. In the

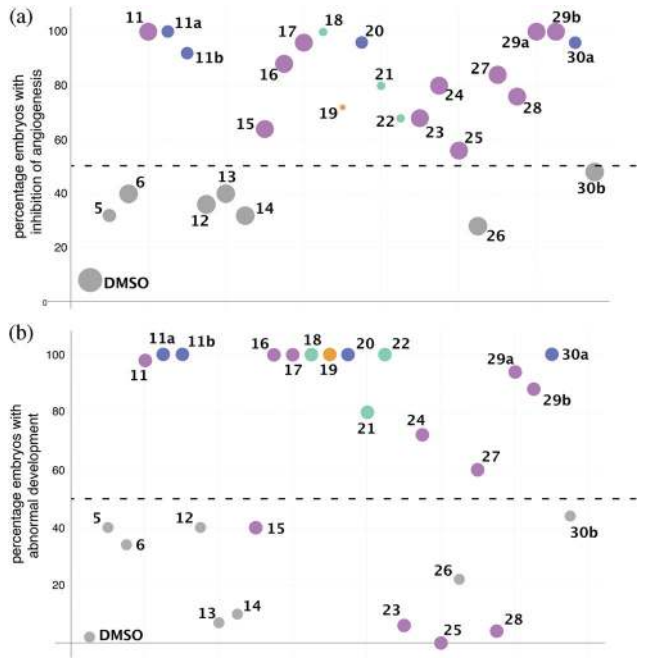

Fig. 3 Structure–activity relationship analysis of noreremophilanes using zebrafish assays. (a) Anti-angiogenic activity assay in zebrafish embryos. 2-day-old embryos exposed to different compounds and the formation of subintestinal vessels (SIVs) assayed at 3 days. The percentage of embryos with complete and/or partial inhibition of angiogenesis is quantified and plotted, n = 25 for each compound. The size of the circle is proportional to the concentration of the compound used for the assay. Embryos were exposed to 50 μM concentration of the compound generally, but where this concentration was lethal, the highest non-lethal concentrations were used *viz*. 25 μM, 12.5 μM, and 6.25 μM. The dotted line represents the 50% mark. The circles are coloured according to the potency of the compounds to block angiogenesis: yellow > green > blue > pink > grey. The x-axis shows the compound number codes. (b) Teratogenicity assay in zebrafish embryos. 6-hour-old zebrafish embryos were exposed to 50 μM compounds and the percentage of embryos with either abnormal development or death at 1 day was quantified and plotted, n = 25. The dotted line represents the 50% mark. The colours of the circles show their potency in inhibiting angiogenesis (from a) for comparison. The x-axis shows the compound number codes.

angiogenesis assay, for compounds that were lethal at 50 μM, a titration was performed and the percentage embryos that showed inhibition of angiogenesis at the highest non-lethal concentrations were quantified and plotted for comparison (Fig. 3a).

Compared to NER**11**, which is a racemic mixture, the enantiomers **11a** and **11b** showed more potent anti-angiogenic activity as both elicited a similar percentage inhibition of angiogenesis at 25 μM as NER**11** did at 50 μM (Fig. 3a). The enantiopure esters with the pantolactone moiety, **29a** & **29b** showed complete inhibition of angiogenesis; there was no difference between the enantiomers. However, enantiomers **30a** & **30b** showed a clear difference in activity with **30a** showing potent anti-angiogenic activity at lower concentrations compared to **30b**. Another observation of interest was that compounds with an angular methyl group such as **5**, **6**, **12**, **14**, **15**, **26** were found to be inferior in anti-angiogenic activity with respect to the corresponding compounds with no angular methyl group. Generally, many potent anti-angiogenic compounds were also toxic at higher concentrations (**11a**, **11b**, **18**, **19**, **20**, **21**, **22**, **30a**), but not all (**11**, **15**, **16**, **17**, **23**, **24**, **25**, **27**, **28**, **29a**, **29b**).

In our teratogenicity assay (Fig. 3b) we observed that there were clearly two groups of compounds, (a) where most embryos (more than 60%) were abnormal and (b) where most embryos (less than 50%) were normal. Based on this screen we found that compounds **11**, **16**, **17**, **18**, **19**, **20**, and **22** containing an ester moiety showed strong bioactivity. Further SAR analysis found that the corresponding acids (**13**, **14**) and amides (**23**, **25**) did not have any significant activity. This information may suggest that esters are readily absorbed by the zebrafish skin rather than the corresponding carboxylic acids. However, the corresponding benzyl amide (**24**) seems to have more bioactivity. Compounds partially saturated with angular hydrogen (**27**) have more activity than the ones partially saturated with an angular methyl group (**5**, **6**, **26**). Fully saturated hydrindane (**28**) has no bioactivity. Enantiopure compounds **11a**, **11b**, **29a** and **29b** were also found to have more adverse effects on embryo survival, with no difference between the enantiomers. However, as in the case of angiogenesis, **30a** & **30b** shows a clear difference in activity. Overall, the tested hydrindane compounds could be generally arranged in a decreasing order of bioactivity on the embryo thus: esters > acids = amides (Fig. 3b).

Teratogenic behaviour of the compounds, in principle, indicates the biological activity of the molecules, which may be explored for therapeutic and laboratory use. However, an ideal anti-angiogenic agent would have minimal side-effects although most anti-angiogenic agents currently in use have other dose-dependent toxicity and side-effects. For example, VEGFR inhibitors and multikinase inhibitors such as regorafenib, that are currently prescribed for anti-cancer therapies, are associated with cardiac problems.[30] So, it is essential to deduce the therapeutic window of the compounds based on their lethal dosage and efficacy.

In our study of NER**11** derivatives, we discovered that compounds such as **11**, **16**, **20**, **18**, and **19** are all potent anti-angiogenic agents. **19** is in fact the most potent angiogenesis inhibitor in our noreremophilane library. However, we discover that all three displayed high anti-angiogenic activity with minimal toxicity (Fig. 3a). In contrast, **23**, **25**, and **28** also show significant anti-angiogenic activity while they are minimally teratogenic.

Noreremophilanes inhibit angiogenesis by inhibiting endothelial tube formation

Anti-angiogenic molecules can inhibit angiogenesis by blocking signals from the milieu or by perturbing tube formation of the endothelial cells. To distinguish between these two possibilities, we picked compound **16**, a racemic compound that had strong anti-angiogenic activity in zebrafish but was not lethal at the concentrations tested, for testing on Human Umbilical Vein Endothelial cells (HUVECs) plated on matrigel.[31] HUVECs when grown on matrigel come together to form tubular structures

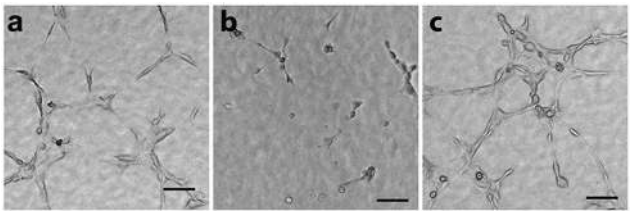

Fig. 4 Noreremophilane scaffold inhibits tubulogenesis in HUVECs. The primary endothelial cells, HUVECs were used to analyse the formation of new vessels. HUVEC cells grown in 2D matrigel were subjected to the tubulogenesis assay (a–c). DMSO (a) and midkine treated cells (c) formed tubules while **16** treated cells showed a breakage of vessel formation (b). Scale bar represents 100 μm.

reminiscent of blood vessels (Fig. 4a). Midkine, a positive regulator of the process stimulates tubulogenesis (Fig. 4c). Treatment of HUVECs with 1 μM of **16** led to a strong inhibition of tubule formation (Fig. 4b). These results indicate that noreremophilane inhibitors affect the endothelial cell autonomously.

Conclusions

Using a combination of synthetic chemistry and rapid *in vivo* screening assays in zebrafish we have identified a noreremophilane with strong anti-angiogenic activity. The noreremophilane scaffold was also found to be very effective at inhibiting tubulogenesis in human endothelial cultures. *In vivo* xenotransplantation assays in zebrafish embryos demonstrate that the compounds may be useful in inhibiting tumor-induced angiogenesis. We synthesized a series of derivatives of the main noreremophilane scaffold and performed SAR analysis in zebrafish embryos to identify moieties that are critical for the anti-angiogenic activity as well as those that are crucial for bioactivity in zebrafish. The power of SAR analysis in live whole organism screens allowed us to identify efficacious compounds while eliminating the toxic ones. Thus, we suggest that combining toxicity and specific activity assays, such as anti-angiogenesis assays, in whole organism screens is a speedy and productive strategy for identifying potentially useful therapeutic agents for human diseases.

Methods & experimental details

Zebrafish lines and maintenance

Fish were bred and maintained as described.[32] All experiments were performed according to protocols approved by the Institutional Animal Ethics Committee (IAEC) of the CSIR-Institute of Genomics and Integrative Biology, India. The zebrafish lines used in this study are *Tg(flk1:EGFP)*[33] that marks the endothelial cells, *Tg(myl7:GAL4-VP16)*[34] that also has a fragment of the myl7 promoter driving GFP in the heart and *Tg(fli1:EGFP::gata1a:DsRed)*[35–37] that was used for visualizing endothelial cells and erythrocytes.

Chemical treatment in zebrafish embryos

Zebrafish embryos were collected from timed matings of adult animals and were staged according to Kimmel *et al.*[38] Embryos were exposed to compounds dissolved in DMSO from 6 to 24 hours for analysis of effects on gross morphology, heart development and other early-stage analysis. For angiogenesis and vasculature assays, the embryos were grown in 0.003% phenylthiourea for depigmentation. Two-day-old embryos were treated with the compounds for 24 hours. Observation and imaging of phenotypes were done using a Zeiss Stemi 2000-C stereomicroscope with an AxiocamICc1 and a Zeiss Axio Scope A1 fluorescence microscope with an AxiocamHRc at appropriate time points.

Wholemount RNA *in situ* hybridization

RNA *in situ* hybridization was performed as previously described.[39] Digoxigenin labelled riboprobes were produced using transcription kits (Roche). The flk1, krox20, otx2, shh, ntl, eve1, pax2a probes were used.

Zebrafish xenotransplantation model

The inhibitory effect of the anti-angiogenic compounds was tested in the tumor microenvironment by injecting DiI-labeled MDA-MB-231 human breast cancer cells in the 2-day-old Tg(fli1:EGFP) zebrafish line near the perivitelline space as described.[29] About 7 nL comprising 100–150 cells mixed with matrigel (1 : 1 dilution) were injected in each anesthetized embryo. The embryos were incubated at 32 °C for 4 hours to increase chances of cancer cell survival. The injected embryos were exposed to compounds in water containing phenylthiourea for 24 h. The blood vessels were visualized 1 day later.

Cellular assays

Human Umbilical Vein Endothelial Cells (HUVECs) were cultured in HiEndoXL™ endothelial cell expansion medium at 37 °C, 5% CO_2 in a gelatin coated T-25 flask. Matrigel was coated in a 48 well culture plate and kept at 37 °C for 30 min. 40 000 cells were plated per well in the 48 well plate. The cells were treated with the control, Midkine and 1 μM of compound **16** in triplicates, and incubated at 37 °C, 5% CO_2 for 4 h. The HUVEC and 0.5% gelatin solution were from HiMedia Laboratories, India. Midkine was procured from Life Technologies-Invitrogen, USA.

General synthesis

All reactions were carried out in oven-dried glassware under a positive pressure of argon or nitrogen unless otherwise mentioned with magnetic stirring. Air sensitive reagents and solutions were transferred *via* a syringe or cannula and were introduced to the apparatus *via* rubber septa. All reagents, starting materials and solvents were obtained from commercial suppliers and used as such without further purification. Reactions were monitored by thin layer chromatography (TLC) with 0.25 mm pre-coated silica gel plates (60 F254). Visualization was accomplished with either UV light or by immersion

in the ethanolic solution of phosphomolybdic acid (PMA), *para*-anisaldehyde, 2,4-DNP, $KMnO_4$ solution or iodine adsorbed on silica gel followed by heating with a heat gun for ~15 s. Column chromatography was performed on silica gel (100–200 or 230–400 mesh size). Deuterated solvents for NMR spectroscopic analyses were used as received. All ^{1}H NMR and ^{13}C NMR spectra were obtained using a 400 MHz or 500 MHz spectrometer. Coupling constants were measured in hertz. Chemical shifts were quoted in ppm, relative to TMS, using the residual solvent peak as a reference standard. The following abbreviations were used to explain the multiplicities: s = singlet, d = doublet, t = triplet, q = quartet, m = multiplet, b = broad. HRMS (ESI) were recorded on an ORBITRAP mass analyser (Thermo Scientific, QExactive). Infrared (IR) spectra were recorded on a FT-IR spectrometer as a thin film. Chemical nomenclature was generated using Chem Bio Draw Ultra 13.0.

Ethyl(3a*S*,4*R*,7a*R*)-2-acetyl-3a,4,5,7a-tetrahydro-1*H*-indene-4-carboxylate (11). To a solution of diene (1.0 g, 8.06 mmol) and ethyl (*E*)-4-oxobut-2-enoate **7** (2.1 g, 16.12 mmol) in dry CH_2Cl_2 (50 mL) was added $BF_3{\cdot}OEt_2$ (1.5 mL, 12.09 mmol) dropwise at −78 °C. The mixture was allowed to warm up to room temperature and was stirred for 4 h at room temperature. The CH_2Cl_2 layer was washed with saturated aqueous $NaHCO_3$ (3 × 15 mL) followed by H_2O (15 mL) and brine (15 mL), dried over anhydrous Na_2SO_4, and concentrated *in vacuo*. The crude material was passed through a small pad of silica gel using 30% EtOAc in petroleum ether as an eluent. The eluent was concentrated and dissolved in EtOH (20 mL), cooled to 0 °C, and treated with 15% ethanolic KOH (10 mL). After stirring for 1 h at room temperature, the reaction mass was evaporated. Water (5 mL) was added and extracted with ethyl acetate (3 × 15 mL). The aqueous layer was acidified with 1 N HCl and extracted with ethyl acetate (3 × 15 mL). The combined organic layers were washed with brine (20 mL), dried over anhydrous Na_2SO_4, and concentrated *in vacuo*. Purification by flash chromatography over silica gel (1.5 : 8.5; EtOAc–petroleum ether) afforded **11** (0.68 g, 36%) as light yellow oil and (4 : 6; EtOAc–petroleum ether) afforded **13** (0.17 g, 10%) as a white solid.

Ethyl(3a*S*,4*R*,7a*R*)-2-acetyl-3a,4,5,7a-tetrahydro-1*H*-indene-4-carboxylate (11). IR ν_{max}(film): 2931, 1730, 1670, 1179 cm^{-1}; ^{1}H NMR (400 MHz, $CDCl_3$) δ 6.70 (s, 1H), 5.74–5.73 (m, 2H), 4.19–4.14 (m, 2H), 3.13–3.09 (m, 1H), 2.91–2.77 (m, 2H), 2.39–2.32 (m, 1H), 2.29 (s, 3H), 2.27–2.17 (m, 3H), 1.26 (t, J = 7.3 Hz, 3H); ^{13}C NMR (100 MHz, $CDCl_3$) δ 197.0, 174.8, 145.6, 145.5, 129.4, 124.7, 60.7, 46.1, 42.0, 37.6, 36.5, 27.2, 26.6, 14.4; HRMS (ESI) m/z calcd for $C_{14}H_{18}O_3$ [M + Na]$^+$ 257.1148, found 257.1147.

(3a*S*,4*R*,7a*R*)-2-Acetyl-3a,4,5,7a-tetrahydro-1*H*-indene-4-carboxylic acid (13). IR ν_{max}(film): 3146, 2934, 1646 cm^{-1}; ^{1}H NMR (400 MHz, $CDCl_3$) δ 6.77 (s, 1H), 5.77–5.76 (m, 2H), 3.18–3.14 (m, 1H), 2.95–2.91 (m, 1H), 2.87–2.80 (m, 1H), 2.47–2.44 (m, 1H), 2.38–2.34 (m, 1H), 2.33 (s, 3H), 2.29–2.22 (m, 2H); ^{13}C NMR (100 MHz, $CDCl_3$) δ 197.3, 180.7, 145.8, 145.4, 129.6, 124.4, 45.8, 41.7, 37.5, 36.6, 26.8, 26.7; HRMS (ESI) m/z calcd for $C_{12}H_{14}O_3$ [M + Na]$^+$ found 229.0835, found 229.0835.

Compounds **12** and **14** were synthesized using the procedure similar to the preparation of **11** and **13**.

Ethyl(3a*S*,4*R*,7a*R*)-2-acetyl-3a-methyl-3a,4,5,7a-tetrahydro-1*H*-indene-4-carboxylate (12). IR ν_{max}(film): 2931, 1730, 1670, 1179 cm^{-1}; ^{1}H NMR (400 MHz, $CDCl_3$) δ 6.76 (s, 1H), 5.76–5.69 (m, 2H), 4.21–4.11 (m, 2H), 2.85 (dd, J = 8.2, 15.8 Hz, 1H), 2.49–2.46 (m, 1H), 2.39–2.35 (m, 1H), 2.31 (s, 3H), 2.31–2.29 (m, 1H), 2.24–2.16 (m, 2H), 1.28 (t, J = 7.3 Hz, 3H), 1.11 (s, 3H); ^{13}C NMR (100 MHz, $CDCl_3$) δ 197.4, 173.8, 152.4, 142.8, 128.0, 124.3, 60.5, 48.3, 47.4, 44.8, 36.6, 26.5, 24.5, 19.8, 14.5; HRMS (ESI) m/z calcd for $C_{15}H_{20}O_3$ [M + Na]$^+$ 271.1305, found 271.1302.

(3a*S*,4*R*,7a*R*)-2-Acetyl-3a-methyl-3a,4,5,7a-tetrahydro-1*H*-indene-4-carboxylic acid (14). IR ν_{max}(film): 3146, 2934, 1646 cm^{-1}; ^{1}H NMR (400 MHz, $CDCl_3$) δ 6.84 (s, 1H), 5.80–5.71 (m, 2H), 2.88 (dd, J = 8.3, 16.1 Hz, 1H), 2.58–2.54 (m, 1H), 2.44–2.39 (m, 1H), 2.34 (s, 3H), 2.32–2.30 (m, 1H), 2.29–2.18 (m, 2H), 1.18 (s, 3H); ^{13}C NMR (100 MHz, $CDCl_3$) δ 197.6, 179.6, 151.9, 143.1, 128.2, 124.0, 48.2, 47.5, 44.7, 36.7, 26.6, 24.5, 19.9; HRMS (ESI) m/z calcd for $C_{13}H_{16}O_3$ [M + Na]$^+$ 243.0992, found 243.0992.

Ethyl(3a*S*,4*R*,7a*S*)-2-acetyl-3a,4,5,6,7,7a-hexahydro-1*H*-indene-4-carboxylate (27). To a solution of compound **11** (30 mg, 0.128 mmol) in dry benzene (5.0 mL) was added Wilkinson's catalyst [$(PPh_3)_3RhCl$] (24 mg, 0.025 mmol). The reaction mixture was degassed by purging argon for 5 min and the flask was then flushed with hydrogen gas to expel the argon. The reaction was allowed to proceed at room temperature under hydrogen balloon pressure for 12 h. Upon completion of the reaction (monitored by TLC), the mixture was concentrated and purified by flash chromatography over silica gel (0.5 : 9.5; EtOAc–petroleum ether) afforded **27** (23 mg, 77%) as colourless oil. IR ν_{max}(film): 2933, 1732, 1670 cm^{-1}; ^{1}H NMR (400 MHz, $CDCl_3$) δ 6.76 (s, 1H), 4.18–4.13 (m, 2H), 2.95–2.91 (m, 1H), 2.53–2.42 (m, 2H), 2.30 (s, 3H), 2.20–2.14 (m, 2H), 1.86–1.77 (m, 2H), 1.61–1.55 (m, 2H), 1.43–1.38 (m, 2H), 1.27 (t, J = 6.9 Hz, 3H); ^{13}C NMR (100 MHz, $CDCl_3$) δ 197.5, 175.3, 147.7, 145.8, 60.6, 46.5, 45.0, 37.3, 33.8, 27.1, 26.5, 26.3, 20.9, 14.3; HRMS (ESI) m/z calcd for $C_{14}H_{20}O_3$ [M + Na]$^+$ 259.1412, found 259.1412.

Ethyl(2*R*,3a*R*,4*R*,7a*S*)-2-acetyloctahydro-1*H*-indene-4-carboxylate (28). To a solution of **11** (50 mg, 0.213 mmol) in EtOAc (5.0 mL) was added PtO_2 (~5 mg) and the mixture was stirred under hydrogen balloon pressure. After 2 h the catalyst was filtered off and concentrated to afford the saturated keto-ester **28** (40 mg, 80% dr-8 : 2) as colourless oil. IR ν_{max}(film): 2931, 1730, 1711 cm^{-1}; ^{1}H NMR (400 MHz, $CDCl_3$) δ 4.15–4.08 (m, 2H), 3.13–2.92 (m, 1H), 2.20–2.17 (m, 2H), 2.15 (s, 3H), 1.99–1.92 (m, 1H), 1.89–1.82 (m, 1H), 1.80–1.68 (m, 4H), 1.54–1.52 (m, 2H), 1.48–1.38 (m, 3H), 1.26–1.22 (m, 3H); ^{13}C NMR (100 MHz, $CDCl_3$) δ 210.8, 176.2, 60.3, 50.4, 43.8, 40.5, 38.6, 32.4, 31.4, 29.2, 27.9, 26.4, 20.5, 14.4; HRMS (ESI) m/z calcd for $C_{14}H_{22}O_3$ [M + Na]$^+$ 261.1461, found 261.1459.

(3a*S*,4*R*,7a*R*)-2-Acetyl-3a,4,5,7a-tetrahydro-1*H*-indene-4-carboxamide (23). To a solution of acid **13** (100 mg, 0.485 mmol)

in dry CH_2Cl_2 (10 mL) was added $(COCl)_2$ (0.08 mL, 0.970 mmol) followed by 1 drop of DMF at 0 °C. The mixture was allowed to stir for 2 h at the same temperature. The solution was concentrated *in vacuo*, to give yellow oil. The crude was dissolved in CH_2Cl_2 (10 mL) and cooled to 0 °C and treated with NH_4OH (25% aqueous solution, 1 mL), the mixture was stirred at room temperature for 2 h and then concentrated. The crude was purified by flash chromatography over silica gel (0.5 : 9.5; MeOH–CH_2Cl_2) which afforded **23** (72 mg, 72%) as a white solid. IR ν_{max}(film): 3470, 1675 cm^{-1}; ^1H NMR (400 MHz, $CDCl_3$) δ 6.76 (s, 1H), 5.83–5.77 (m, 2H), 5.67–5.61 (m, 2H), 3.15–3.11 (m, 1H), 2.92–2.79 (m, 2H), 2.31 (s, 3H), 2.26–2.15 (m, 4H); ^{13}C NMR (100 MHz, $CDCl_3$) δ 197.3, 176.9, 145.7, 145.6, 129.5, 124.8, 46.4, 43.5, 37.8, 36.5, 28.2, 26.7; HRMS (ESI) *m*/*z* calcd for $C_{12}H_{15}O_2N$ $[M + Na]^+$ 228.0995, found 228.0994.

Compounds **16**, **17**, **18**, **19**, **20**, **21**, **22**, **24** and **25** were synthesized using the procedure similar to compound **23**.

Isobutyl(3a*S*,4*R*,7a*R*)-2-acetyl-3a,4,5,7a-tetrahydro-1*H*-indene-4-carboxylate (16). (Yield: 73%); IR ν_{max}(film): 2931, 1732, 1671 cm^{-1}; ^1H NMR (400 MHz, $CDCl_3$) δ 6.72 (s, 1H), 5.76–5.75 (m, 2H), 3.93–3.89 (m, 2H), 3.16–3.12 (m, 1H), 2.92–2.79 (m, 2H), 2.43–2.37 (m, 1H), 2.31 (s, 3H), 2.25–2.22 (m, 3H), 1.98–1.92 (m, 1H), 0.95 (d, *J* = 6.8 Hz, 6H); ^{13}C NMR (100 MHz, $CDCl_3$) δ 197.1, 174.9, 145.8, 145.6, 129.5, 124.7, 70.9, 46.1, 42.1, 37.7, 36.5, 27.9, 27.3, 26.6, 19.2 (2C); HRMS (ESI) *m*/*z* calcd for $C_{16}H_{22}O_3$ $[M + Na]^+$ 285.1461, found 285.1461.

Butyl(3a*S*,4*R*,7a*R*)-2-acetyl-3a,4,5,7a-tetrahydro-1*H*-indene-4-carboxylate (17). (Yield: 71%); IR ν_{max}(film): 2931, 1730, 1670, 1179 cm^{-1}; ^1H NMR (400 MHz, $CDCl_3$) δ 6.71 (s, 1H), 5.76–5.75 (m, 2H), 4.15–4.11 (m, 2H), 3.14–3.10 (m, 1H), 2.93–2.79 (m, 2H), 2.41–2.37 (m, 1H), 2.30 (s, 3H), 2.23–2.19 (m, 2H), 1.64–1.61 (m, 3H), 1.42–1.36 (m, 2H), 0.94 (t, *J* = 7.3 Hz, 3H); ^{13}C NMR (100 MHz, $CDCl_3$) δ 197.1, 174.9, 145.8, 145.6, 129.4, 124.7, 64.7, 46.1, 42.1, 37.7, 36.5, 30.8, 27.2, 26.6, 19.3, 13.8; HRMS (ESI) *m*/*z* calcd for $C_{16}H_{22}O_3$ $[M + Na]^+$ 285.1461, found 285.1460.

Benzyl(3a*S*,4*R*,7a*R*)-2-acetyl-3a,4,5,7a-tetrahydro-1*H*-indene-4-carboxylate (18). (Yield: 76%); IR ν_{max}(film): 2931, 1730, 1670, 1179 cm^{-1}; ^1H NMR (400 MHz, $CDCl_3$) δ 7.37–7.33 (m, 5H), 6.61 (s, 1H), 5.78–5.76 (m, 2H), 5.23–5.12 (m, 2H), 3.15–3.10 (m, 1H), 2.93–2.77 (m, 2H), 2.46–2.40 (m, 1H), 2.36–2.30 (m, 1H), 2.26–2.25 (m, 1H), 2.24 (s, 3H), 2.21–2.18 (m, 1H); ^{13}C NMR (100 MHz, $CDCl_3$) δ 197.1, 174.6, 145.6 (2C), 136.0, 129.4, 128.8 (2C), 128.6, 128.3 (2C), 124.6, 66.5, 46.2, 42.1, 37.7, 36.4, 27.1, 26.6; HRMS (ESI) *m*/*z* calcd for $C_{19}H_{20}O_3$ $[M + Na]^+$ 319.1305, found 319.1304.

2,2,2-Trifluoroethyl(3a*S*,4*R*,7a*R*)-2-acetyl-3a,4,5,7a-tetrahydro-1*H*-indene-4-carboxylate (19). (Yield: 71%); IR ν_{max}(film): 1728, 1668 cm^{-1}; ^1H NMR (400 MHz, $CDCl_3$) δ 6.68 (s, 1H), 5.80–5.73 (m, 2H), 4.61–4.43 (m, 2H), 3.16–3.12, (m, 1H), 2.96–2.81 (m, 2H), 2.54–2.48 (m, 1H), 2.38–2.32 (m, 1H), 2.30 (s, 3H), 2.28–2.22 (m, 2H); ^{13}C NMR (100 MHz, $CDCl_3$) δ 197.0, 173.3, 146.0, 144.6, 129.5, 124.2, 121.7, 61.4 (q, 1C, *J* = 36.2 Hz), 46.1, 41.7, 37.7, 36.4, 26.8, 26.6; HRMS (ESI) *m*/*z* calcd for $C_{14}H_{15}O_3F_3$ $[M + Na]^+$ 311.0866, found 311.0862.

Cyclopropyl methyl(3a*S*,4*R*,7a*R*)-2-acetyl-3a,4,5,7a-tetrahydro-1*H*-indene-4-carboxylate (20). (Yield: 64%); IR ν_{max}(film):1730, 1663 cm^{-1}; ^1H NMR (400 MHz, $CDCl_3$) δ 6.73 (s, 1H), 5.78–5.72 (m, 2H), 4.00–3.90 (m, 2H), 3.13–3.09, (m, 1H), 2.90–2.78 (m, 2H), 2.41–2.35 (m, 1H), 2.33–2.28 (m, 1H), 2.30 (s, 3H), 2.26–2.19 (m, 2H), 1.16–1.11 (m, 1H), 0.59–0.54 (m, 2H), 0.30–0.26 (m, 2H); ^{13}C NMR (100 MHz, $CDCl_3$) δ 197.1, 174.9, 145.7, 145.5, 129.3, 124.7, 69.4, 46.2, 42.1, 37.7, 36.4, 27.2, 26.6, 9.9, 3.3 (2C); HRMS (ESI) *m*/*z* calcd for $C_{16}H_{20}O_3$ $[M + Na]^+$ 283.1305, found 283.1303.

Cyclohexyl methyl(3a*S*,4*R*,7a*R*)-2-acetyl-3a,4,5,7a-tetrahydro-1*H*-indene-4-carboxylate (21). (Yield: 68%); IR ν_{max}(film): 2931, 1732, 1671 cm^{-1}; ^1H NMR (400 MHz, $CDCl_3$) δ 6.71 (s, 1H), 5.75 (m, 2H), 3.93 (d, *J* = 6.4 Hz, 2H), 3.44–3.42 (m, 1H), 3.14–3.09 (m, 1H), 2.90–2.78 (m, 2H), 2.40–2.34 (m, 1H), 2.30 (s, 3H), 2.32–2.25 (m, 1H), 2.24–2.17 (m, 2H), 1.74–1.71 (m, 4H), 1.24–1.20 (m, 4H), 1.02–.093 (m, 2H); ^{13}C NMR (100 MHz, $CDCl_3$) δ 197.1, 174.9, 145.8, 145.5, 129.4, 124.7, 70.0, 68.9, 46.2, 42.1, 40.6, 37.7, 37.3, 36.5, 29.8, 27.2, 26.4, 25.9, 25.7; HRMS (ESI) *m*/*z* calcd for $C_{19}H_{26}O_3$ $[M + Na]^+$ 325.1774, found 325.1772.

Allyl(3a*S*,4*R*,7a*R*)-2-acetyl-3a,4,5,7a-tetrahydro-1*H*-indene-4-carboxylate (22). (Yield: 66%); IR ν_{max}(film): 2930, 1730, 1669 cm^{-1}; ^1H NMR (400 MHz, $CDCl_3$) δ 6.71 (s, 1H), 5.96–5.89 (m, 1H), 5.76 (m, 2H), 5.33 (dd, *J* = 1.2, 17.1 Hz, 1H), 5.25 (dd, *J* = 1.2, 10.5 Hz, 1H), 4.63 (d, *J* = 5.1 Hz, 2H), 3.16–3.12 (m, 1H), 2.92–2.79 (m, 2H), 2.45–2.39 (m, 1H), 2.35–2.29 (m, 1H), 2.30 (s, 3H), 2.27–2.21 (m, 2H); ^{13}C NMR (100 MHz, $CDCl_3$) δ 197.1, 174.5, 145.6, 145.6, 132.2, 129.5, 124.6, 118.5, 65.4, 46.1, 42.0, 37.7, 36.5, 27.2, 26.6; HRMS (ESI) *m*/*z* calcd for $C_{15}H_{18}O_3$ $[M + Na]^+$ 269.1148, found 269.1147.

(3a*S*,4*R*,7a*R*)-2-Acetyl-*N*-benzyl-3a,4,5,7a-tetrahydro-1*H*-indene-4-carboxamide (24). (Yield: 80%); IR ν_{max}(film): 2931, 1670, 1179 cm^{-1}; ^1H NMR (400 MHz, $CDCl_3$) δ 7.35–7.28 (m, 5H), 6.65 (s, 1H), 6.04 (bs, 1H), 5.77–5.76 (m, 2H), 4.57–4.52 (m, 1H), 4.40–4.35 (m, 1H), 3.16–3.12 (m, 1H), 2.89–2.75 (m, 2H), 2.28–2.25 (m, 1H), 2.20 (s, 3H), 2.17–2.04 (m, 3H); ^{13}C NMR (100 MHz, $CDCl_3$) δ 197.2, 174.3, 146.0, 145.5, 138.5, 129.2, 128.9 (2C), 127.8 (2C), 127.7, 125.1, 46.6, 44.3, 43.6, 37.9, 36.4, 28.2, 26.5; HRMS (ESI) *m*/*z* calcd for $C_{19}H_{21}O_2N$ $[M + Na]^+$ 318.1465, found 318.1462.

(3a*S*,4*R*,7a*R*)-2-Acetyl-*N*,*N*-diethyl-3a,4,5,7a-tetrahydro-1*H*-indene-4-carboxamide (25). (Yield: 74%); IR ν_{max}(film): 2931, 1670, 1179 cm^{-1}; ^1H NMR (400 MHz, $CDCl_3$) δ 6.66 (s, 1H), 5.83–5.79 (m, 2H), 3.50–3.45 (m, 1H), 3.36–3.18 (m, 4H), 2.90–2.80 (m, 2H), 2.42–2.35 (m, 1H), 2.26 (s, 3H), 2.24–2.17 (m, 2H), 2.11–2.06 (m, 1H), 1.14–1.06 (m, 6H); ^{13}C NMR (100 MHz, $CDCl_3$) δ 197.2, 173.7, 146.6, 145.3, 129.1, 125.4, 47.0, 42.0, 40.6, 39.2, 38.0, 36.4, 28.7, 26.6, 15.2, 13.3; HRMS (ESI) *m*/*z* calcd for $C_{16}H_{23}O_2N$ $[M + Na]^+$ 284.1621, found 284.1620.

Ethyl(3a*S*,4*R*,7a*S*)-2-acetyl-3a-methyl-3a,4,5,6,7,7a-hexa hydro-1*H*-indene-4-carboxylate (26). Compound **26** was synthesized using the procedure similar to the preparation of **27**.

IR ν_{max}(film): 2933, 1732, 1670 cm^{-1}; ^1H NMR (400 MHz, $CDCl_3$) δ 6.84 (s, 1H), 4.20–4.09 (m, 2H), 2.49 (dd, J = 8.1, 15.8 Hz, 1H), 2.43–2.36 (m, 1H), 2.31 (s, 3H), 2.30–2.27 (m, 1H), 2.05–1.99 (m, 1H), 1.73–1.63 (m, 3H), 1.60–1.53 (m, 1H), 1.50–1.36 (m, 2H), 1.28 (t, J = 7.1 Hz, 3H), 1.12 (s, 3H); ^{13}C NMR (100 MHz, $CDCl_3$) δ 197.9, 174.5, 154.6, 142.7, 60.3, 48.9, 48.6, 46.6, 33.2, 26.4, 24.0, 23.1, 20.9, 19.3, 14.5; HRMS (ESI) m/z calcd for $C_{15}H_{22}O_3$ $[M + Na]^+$ 273.1461, found 273.1460.

(3a*S*,4*R*,7a*S*)-2-Acetyl-3a-methyl-3a,4,5,6,7,7a-hexahydro-1*H*-indene-4-carboxylic acid (6). To a solution of **26** (35 mg, 0.14 mmol) in EtOH (2 mL) and water (2 mL) was added lithium hydroxide monohydrate (12 mg, 0.28 mmol) at 0 °C. The mixture was warmed up to room temperature and stirred for 12 h. The mixture was acidified to pH 2 with 1 N HCl. The volatiles were evaporated and the residue was extracted with EtOAc (2 × 5 mL). The combined organic layer was washed with brine (3 mL), dried over anhydrous Na_2SO_4, and concentrated *in vacuo*. Purification by flash chromatography over silica gel (3.0 : 7.0; EtOAc–petroleum ether) afforded **6** (30 mg, 96%) as a white solid. IR ν_{max}(film): 3144, 2936, 1646 cm^{-1}; ^1H NMR (400 MHz, $CDCl_3$) δ 6.93 (s, 1H), 2.52 (dd, J = 8.2, 16.0 Hz, 1H), 2.45–2.36 (m, 2H), 2.34 (s, 3H), 2.09–2.05 (m, 1H), 1.78–1.76 (m, 1H), 1.69–1.66 (m, 2H), 1.62–1.57 (m, 1H), 1.50–1.42 (m, 2H), 1.20 (s, 3H); ^{13}C NMR (100 MHz, $CDCl_3$) δ 198.2, 180.7, 154.3, 143.0, 48.7, 48.5, 46.6, 33.2, 26.5, 23.9, 22.9, 20.7, 19.3; HRMS (ESI) m/z calcd for $C_{13}H_{18}O_3$ $[M + Na]^+$ 245.1148, found 245.1146.

Methyl(3a*S*,4*R*,7a*R*)-2-acetyl-3a-methyl-3a,4,5,7a-tetrahydro-1*H*-indene-4-carboxylate (15). Compound **15** was synthesized using the procedure similar to the preparation of **23**. (Yield: 72%); IR ν_{max}(film): 2930, 1732, 1671 cm^{-1}; ^1H NMR (400 MHz, $CDCl_3$) δ 6.75 (s, 1H), 5.76–5.69 (m, 2H), 3.70 (s, 3H), 2.86 (dd, J = 8.2, 15.9 Hz, 1H), 2.52–2.49 (m, 1H), 2.40–2.36 (m, 1H), 2.32 (s, 3H), 2.30–2.17 (m, 3H), 1.12 (s, 3H); ^{13}C NMR (100 MHz, $CDCl_3$) δ 197.5, 174.3, 152.1, 143.0, 128.1, 124.2, 57.7, 48.3, 47.4, 44.8, 36.6, 26.6, 24.7, 19.9; HRMS (ESI) m/z calcd for $C_{14}H_{18}O_3$ $[M + Na]^+$ 257.1148, found 257.1147.

Methyl(3a*S*,4*R*,7a*S*)-2-acetyl-3a-methyl-3a,4,5,6,7,7a-hexahydro-1*H*-indene-4-carboxylate (5). Compound **5** was synthesized using the procedure similar to the preparation of **27**. (Yield: 70%); IR ν_{max}(film): 1720, 1668 cm^{-1}; ^1H NMR (400 MHz, $CDCl_3$) δ 6.83 (s, 1H), 3.70 (s, 3H), 2.51 (dd, J = 8.1, 16.1 Hz, 1H), 2.44–2.37 (m, 1H), 2.32 (s, 3H), 2.06–2.00 (m, 1H), 1.76–1.72 (m, 1H), 1.66–1.64 (m, 2H), 1.57–1.54 (m, 2H), 1.52–1.49 (m, 1H), 1.45–1.41 (m, 1H), 1.12 (s, 3H); ^{13}C NMR (100 MHz, $CDCl_3$) δ 197.9, 175.0, 154.3, 142.9, 51.6, 48.9, 48.7, 46.6, 33.4, 26.5, 24.0, 23.2, 20.9, 19.5.

Synthesis of enantiopure noreremophilane derivatives

To a solution of *rac*-**13** (300 mg, 1.46 mmol) in dry CH_2Cl_2 (20 mL) under a nitrogen atmosphere were added D-(−) pantolactone (190 mg, 1.46 mmol), HOBT (296 mg, 2.19 mmol), EDC·HCl (420 mg, 2.19 mmol) and DIPEA (0.4 mL, 2.19 mmol) at room temperature. The reaction mixture was allowed to stir at room temperature for 12 h. The mixture was washed with saturated aqueous $NaHCO_3$ (5 mL) and brine (5 mL). The organic layer was dried over anhydrous Na_2SO_4, concentrated *in vacuo*. Purification by flash chromatography over silica gel (2.0 : 8.0; EtOAc–petroleum ether) afforded **29a** (143 mg, 31%) and **29b** (120 mg, 26%) as white solids.

(*R*)-4,4-Dimethyl-2-oxotetrahydrofuran-3-yl(3a*S*,4*R*,7a*R*)-2-acetyl-3a,4,5,7a-tetrahydro-1*H*-indene-4-carboxylate (29a). IR ν_{max}(film): 1720, 1668 cm^{-1}; ^1H NMR (400 MHz, $CDCl_3$) δ 6.93 (s, 1H), 5.82–5.78 (m, 2H), 5.44 (s, 1H), 4.09–4.04 (m, 2H), 3.38–3.33 (m, 1H), 2.98–2.92 (m, 1H), 2.88–2.82 (m, 1H), 2.58–2.52 (m, 1H), 2.34 (s, 3H), 2.32–2.31 (m, 2H), 2.29–2.22 (m, 1H), 1.21 (s, 3H), 1.12 (s, 3H); ^{13}C NMR (100 MHz, $CDCl_3$) δ 197.4, 174.1, 172.4, 145.7, 145.5, 129.7, 124.2, 76.4, 75.3, 46.8, 41.8, 40.3, 37.8, 36.4, 26.8, 26.6, 23.1, 20.1; HRMS (ESI) m/z calcd for $C_{18}H_{22}O_5$ $[M + Na]^+$ 341.1359, found 341.1357. $[\alpha]_D^{25}$ = +9.70 (c = 1.30, $CHCl_3$).

(*R*)-4,4-Dimethyl-2-oxotetrahydrofuran-3-yl(3a*R*,4*S*,7a*S*)-2-acetyl-3a,4,5,7a-tetrahydro-1*H*-indene-4-carboxylate (29b). IR ν_{max}(film): 1720, 1668 cm^{-1}; ^1H NMR (400 MHz, $CDCl_3$) δ 6.78 (s, 1H), 5.78 (s, 2H), 5.40 (s, 1H), 4.09–4.03 (d, J = 3.2 Hz, 2H), 3.22–3.18 (m, 1H), 2.96–2.81 (m, 2H), 2.57–2.51 (m, 1H), 2.44–2.38 (m, 1H), 2.31 (s, 3H), 2.30–2.23 (m, 2H), 1.23 (s, 3H), 1.13 (s, 3H); ^{13}C NMR (100 MHz, $CDCl_3$) δ 197.0, 173.5, 172.2, 145.9, 145.0, 129.5, 124.5, 76.3, 75.3, 46.0, 42.2, 40.2, 37.7, 36.5, 27.3, 26.7, 23.2, 20.1; HRMS (ESI) m/z calcd for $C_{18}H_{22}O_5$ $[M + Na]^+$ 341.1359, found 341.1354; $[\alpha]_D^{25}$ = −11.05 (c = 2.90, $CHCl_3$).

Ethyl(3a*S*,4*R*,7a*R*)-2-acetyl-3a,4,5,7a-tetrahydro-1*H*-indene-4-carboxylate (11a). (Yield: 59%); ^1H NMR (400 MHz, $CDCl_3$) δ 6.72 (s, 1H), 5.78–5.76 (m, 2H), 4.21–4.16 (m, 2H), 3.15–3.11 (m, 1H), 2.94–2.79 (m, 2H), 2.41–2.35 (m, 1H), 2.31 (s, 3H), 2.27–2.17 (m, 3H), 1.28 (t, J = 7.3 Hz, 3H); ^{13}C NMR (100 MHz, $CDCl_3$) δ 197.1, 174.8, 145.7, 145.6, 129.5, 124.7, 60.8, 46.1, 42.1, 37.7, 36.5, 27.2, 26.7, 14.1; HRMS (ESI) m/z calcd for $C_{14}H_{18}O_3$ $[M + Na]^+$ 257.1148, found 257.1147; $[\alpha]_D^{25.4}$ = +20.87 (c = 1.0, $CHCl_3$).

Propyl(3a*S*,4*R*,7a*R*)-2-acetyl-3a,4,5,7a-tetrahydro-1*H*-indene-4-carboxylate (30a). (Yield: 55%); ^1H NMR (400 MHz, $CDCl_3$) δ 6.72 (s, 1H), 5.77 (m, 2H), 4.09 (t, J = 6.8 Hz, 2H), 3.16–3.11 (m, 1H), 2.90–2.79 (m, 2H), 2.42–2.33 (m, 2H), 2.31 (s, 3H), 2.29–2.18 (m, 2H), 1.72–1.63 (m, 2H), 0.96 (t, J = 7.8 Hz, 3H); ^{13}C NMR (100 MHz, $CDCl_3$) δ 197.1, 174.9, 144.7, 145.5, 129.5, 124.7, 66.4, 46.1, 42.1, 37.7, 36.5, 27.3, 26.7, 22.2, 10.6; HRMS (ESI) m/z calcd for $C_{15}H_{20}O_3$ $[M + Na]^+$ 271.1305, found 271.1306; $[\alpha]_D^{25}$ = +18.42 (c = 0.9, $CHCl_3$).

Ethyl(3a*R*,4*S*,7a*S*)-2-acetyl-3a,4,5,7a-tetrahydro-1*H*-indene-4-carboxylate (11b). (Yield: 56%); ^1H NMR (400 MHz, $CDCl_3$) δ 6.72 (s, 1H), 5.78–5.76 (m, 2H), 4.21–4.16 (m, 2H), 3.15–3.11 (m, 1H), 2.94–2.79 (m, 2H), 2.41–2.35 (m, 1H), 2.31 (s, 3H), 2.27–2.17 (m, 3H), 1.28 (t, J = 7.3 Hz, 3H); ^{13}C NMR (100 MHz, $CDCl_3$) δ 197.1, 174.8, 145.7, 145.6, 129.5, 124.7, 60.8, 46.1, 42.1, 37.7, 36.5, 27.2, 26.7, 14.1; HRMS (ESI) m/z calcd for $C_{14}H_{18}O_3$ $[M + Na]^+$ 257.1148, found 257.1146; $[\alpha]_D^{25}$ = −21.92 (c = 1.0, $CHCl_3$).

Propyl(3a*R*,4*S*,7a*S*)-2-acetyl-3a,4,5,7a-tetrahydro-1*H*-indene-4-carboxylate (30b). (Yield: 50%); ^1H NMR (400 MHz, $CDCl_3$)

δ 6.72 (s, 1H), 5.77 (m, 2H), 4.09 (t, J = 6.8 Hz, 2H), 3.16–3.11 (m, 1H), 2.90–2.79 (m, 2H), 2.42–2.33 (m, 2H), 2.31 (s, 3H), 2.29–2.18 (m, 2H), 1.72–1.63 (m, 2H), 0.96 (t, J = 7.8 Hz, 3H); ^{13}C NMR (100 MHz, $CDCl_3$) δ 197.1, 174.9, 144.7, 145.5, 129.5, 124.7, 66.4, 46.1, 42.1, 37.7, 36.5, 27.3, 26.7, 22.2, 10.6; HRMS (ESI) m/z calcd for $C_{15}H_{20}O_3$ $[M + Na]^+$ 271.1305, found 271.1305; $[\alpha]_D^{25} = -15.37$ (c = 0.5, $CHCl_3$).

Acknowledgements

The Council of Scientific and Industrial Research (CSIR), New Delhi is acknowledged for the financial support through NCL-IGIB Joint Research Initiative (BSC0124). DSR acknowledges the Ministry of Earth Sciences (MOES, New Delhi) for the financial support under the program "Drugs from Sea". KLH thanks CSIR, New Delhi, for the award of a research fellowship. SS acknowledges financial support from BioCARe Department of Biotechnology. NK is supported by a fellowship from Shiv Nadar University. Thanks to Avinash Bajaj and Somnath Kundu, Regional Centre for Biotechnology, Faridabad for the kind gift of DiI-labeled MDA-MB-231 cells and thanks to Ajith Nair, Towa optics, India Pvt Ltd for help in image processing using IMARIS software.

Notes and references

1 D. J. Newman, G. M. Cragg and K. M. Snader, *J. Nat. Prod.*, 2003, **66**, 1022.
2 S. Basu and C. Sachidanandan, *Chem. Rev.*, 2013, **113**, 7952.
3 R. T. Peterson and M. C. Fishman, *Methods Cell Biol.*, 2011, **105**, 525.
4 E. Gebruers, M. L. Cordero-Maldonado, A. I. Gray, C. Clements, A. L. Harvey, R. Edrada-Ebel, P. A. de Witte, A. D. Crawford and C. V. Esguerra, *PLoS One*, 2013, **8**, e83293.
5 S. K. Reddy Guduru, S. Chamakuri, G. Chandrasekar, S. S. Kitambi and P. Arya, *ACS Med. Chem. Lett.*, 2013, **4**, 666.
6 W. Zhao, Q. Ye, X. Tan, H. Jiang, X. Li, K. Chen and A. D. Kinghorn, *J. Nat. Prod.*, 2001, **64**, 1196.
7 T. Shen, P. L. Li, C. S. Yuan and Z. J. Jia, *Acta Chim. Sin.*, 2007, **65**, 1638.
8 T. Yamada, M. Doi, A. Miura, W. Harada, M. Hiramura, K. Minoura, R. Tanaka and A. Numata, *J. Antibiot.*, 2005, **58**, 185.
9 T. S. Wu, M. S. Kao, P. L. Wu, F. W. Lin, L. S. Shi, M. J. Liou and C. Y. Li, *Chem. Pharm. Bull.*, 1999, **47**, 375.
10 T. S. Wu, M. S. Kao, P. L. Wu, F. W. Lin, L. S. Shi and C. M. Teng, *Phytochemistry*, 1999, **52**, 901.
11 D. S. Reddy, *Org. Lett.*, 2004, **6**, 3345.
12 K. L. Handore and D. S. Reddy, *Org. Lett.*, 2013, **15**, 1894.
13 K. L. Handore, B. Seetharamsingh and D. S. Reddy, *J. Org. Chem.*, 2013, **78**, 8149.
14 Z. H. He, M. F. He, S. C. Ma and P. P. But, *J. Ethnopharmacol.*, 2009, **121**, 313.
15 X. Dong, Z. C. Han and R. Yang, *Crit. Rev. Oncol. Hematol.*, 2007, **62**, 105.
16 R. Bicknell, *Br. J. Cancer*, 2005, **92**(Suppl 1), S2–5.
17 P. V. Bonnesen, C. L. Puckett, R. V. Honeychuck and W. H. Hersh, *J. Am. Chem. Soc.*, 1989, **111**, 6070.
18 Y. Hashimoto, T. Nagashima, K. Kobayashi, M. Hasegawa and K. Saigo, *Tetrahedron*, 1993, **49**, 6349.
19 J. D. Winkler, H. S. Kim, S. Kim, C. S. Penkett, S. K. Bhattacharya, K. Ando and K. N. Houk, *J. Org. Chem.*, 1997, **62**, 2957.
20 L. C. Baillie, A. Batsanov, J. R. Bearder and D. A. Whiting, *J. Chem. Soc., Perkin Trans. 1*, 1998, 3471.
21 M. Ge, B. M. Stoltz and E. J. Corey, *Org. Lett.*, 2000, **2**, 1927.
22 D. S. Reddy and S. A. Kozmin, *J. Org. Chem.*, 2004, **69**, 4860.
23 G. A. Kraus and J. J. Kim, *Org. Lett.*, 2004, **6**, 3115.
24 J. Sauer, *Angew. Chem., Int. Ed. Engl.*, 1967, **6**, 16.
25 K. N. Houk and R. W. Strozier, *J. Am. Chem. Soc.*, 1973, **95**, 4094.
26 K. N. Houk, *Acc. Chem. Res.*, 1975, **8**, 361.
27 O. Eisenstein, J. M. LeFour, N. T. Anh and R. F. Hudson, *Tetrahedron*, 1977, **33**, 523.
28 Y. Zhao, Z. Jia and H. Peng, *J. Nat. Prod.*, 1995, **58**, 1358.
29 S. Nicoli and M. Presta, *Nat. Protocols*, 2007, **2**, 2918.
30 G. Chimote, J. Sreenivasan, N. Pawar, J. Subramanian, H. Sivaramakrishnan and S. Sharma, *Drug Des., Dev. Ther.*, 2014, **8**, 1107.
31 M. L. Ponce, *Methods Mol. Biol.*, 2009, **467**, 183.
32 M. Westerfield, *The zebrafish book. A guide for the laboratory use of zebrafish (Danio rerio)*, Univ. of Oregon Press, Eugene, 4th edn, 2000.
33 S. W. Jin, D. Beis, T. Mitchell, J. N. Chen and D. Y. Stainier, *Development*, 2005, **132**, 5199.
34 A. U. Steinbicker, C. Sachidanandan, A. J. Vonner, R. Z. Yusuf, D. Y. Deng, C. S. Lai, K. M. Rauwerdink, J. C. Winn, B. Saez, C. M. Cook, B. A. Szekely, C. N. Roy, J. S. Seehra, G. D. Cuny, D. T. Scadden, R. T. Peterson, K. D. Bloch and P. B. Yu, *Blood*, 2011, **117**, 4915.
35 M. K. Lalwani, M. Sharma, A. R. Singh, R. K. Chauhan, A. Patowary, N. Singh, V. Scaria and S. Sivasubbu, *PLoS One*, 2012, **7**, e52588.
36 D. Traver, B. H. Paw, K. D. Poss, W. T. Penberthy, S. Lin and L. I. Zon, *Nat. Immunol.*, 2003, **4**, 1238.
37 N. D. Lawson and B. M. Weinstein, *Dev. Biol.*, 2002, **248**, 307.
38 C. B. Kimmel, W. W. Ballard, S. R. Kimmel, B. Ullmann and T. F. Schilling, Stages of embryonic development of the zebrafish, *Dev. Dyn.*, 1995, **203**, 253.
39 D. Henrique, J. Adam, A. Myat, A. Chitnis, J. Lewis and D. Ish-Horowicz, *Nature*, 1995, **375**, 787.

